Journal of Power Sources 210 (2012) 146–153

Contents lists available at SciVerse ScienceDirect

Journal of Power Sources

journal homepage: www.elsevier.com/locate/jpowsour

Role of silver current collector on the operational stability of selected cobalt-containing oxide electrodes for oxygen reduction reaction

Yubo Chen [a], Fucun Wang [a], Dengjie Chen [a], Feifei Dong [a], Hee Jung Park [b,*], Chan Kwak [b], Zongping Shao [a,*]

[a] State Key Laboratory of Materials-Oriented Chemical Engineering, College of Chemistry & Chemical Engineering, Nanjing University of Technology, China
[b] Samsung Advanced Institute of Technology (SAIT), 14-1 Nongseo-dong, Yongin-si, Gyunggi-do 446-712, Republic of Korea

ARTICLE INFO

Article history:
Received 28 December 2011
Received in revised form 6 March 2012
Accepted 9 March 2012
Available online 21 March 2012

Keywords:
Solid oxide fuel cells
Current collector
Oxygen reduction reaction
Long-term stability
Silver

ABSTRACT

The long-term stability for oxygen reduction reaction (ORR) of two typical perovskite cathode materials of SOFCs, i.e., $Ba_{0.5}Sr_{0.5}Co_{0.8}Fe_{0.2}O_{3-\delta}$ (BSCF) and $Sm_{0.5}Sr_{0.5}CoO_{3-\delta}$ (SSC), is investigated in a symmetric cell configuration under air condition at 700 °C using $Sm_{0.2}Ce_{0.8}O_{1.9}$ (SDC) electrolyte substrate and silver current collectors. Moreover, two different methods of silver current collection are tested, i.e., whole electrode surface deposited with a diluted silver paste (CC-01) and a mesh-like current collector using concentrated silver paste (CC-02). Electrochemical impedance spectra are applied for stability investigations. With the CC-01 current collector, the performance of the electrode deteriorates significantly, although the initial performance is good. By contrast, fairly stable performance is obtained from symmetric cells with either BSCF or SSC + SDC electrodes using the CC-02 current collector, even though a phase transition is observed for BSCF. For instance, after approximately 800 h of continuous stability testing, the area-specific resistance of the BSCF electrode retains a value of approximately 0.065 $\Omega\,cm^2$, except for a slight fluctuation within the range of 0.06–0.07 $\Omega\,cm^2$. These findings reveal that both BSCF and SSC can be stably operated for ORR under symmetric cell conditions; however, an appropriate current collection method is crucial to achieving stable performance.

1. Introduction

Solid-oxide fuel cells (SOFCs) are ideal devices for clean power generation in the future due to their high efficiency, low emissions and fuel flexibility. However, for this attractive technology to become practical for widespread application, several important requirements must be satisfied, such as sufficiently long lifetime, high power output and materials and operational costs low enough to compete with current existing power generation technologies such as combustion power plants. Reducing the operating temperature to an intermediate range, i.e., 500–800 °C, is believed to be important for the commercialization of SOFC technology because it can potentially increase cell lifetime and reduce materials and operational costs [1,2]. However, at reduced temperatures, low cell power output has become an emerging problem for fuel cells with thin-film electrolyte due to sluggish cathode activity for the oxygen reduction reaction (ORR). The reaction rate often decreases markedly with decreasing operating temperature due to the large activation energy associated with the ORR, which is typically higher than 110 kJ mol^{-1} [3,4]. On the other hand, the ORR is closely related to the electrode-electrolyte-air triple phase boundary (TPB) [5]. An increase in TPB length may effectively increase the low-temperature performance of SOFC cathodes by increasing the ORR rate. By applying mixed oxygen ionic and electronic conducting electrodes, the electro-active sites can extend to the region several to tens of micrometers away from the TPB, in some cases to the entire exposed surface of the electrode (typically for electrodes with very high oxygen-ionic conductivity, such as $Ba_{0.5}Sr_{0.5}Co_{0.8}Fe_{0.2}O_{3-\delta}$ (BSCF) electrode [6]). As a result, the performance of BSCF electrode for ORR at reduced temperature is significantly improved compared with the state-of-the-art $La_{0.8}Sr_{0.2}MnO_3$ electrode, which is an electronic conductor with negligible ionic conductivity before current polarization, although the activation energy for ORR does not change significantly. For example, in a symmetric cell test, area specific resistance (ASR) as low as 0.07 $\Omega\,cm^2$ was reported for a BSCF electrode for ORR at 600 °C [7]. Currently, considerable research is aimed at using mixed conducting oxides as oxygen reduction electrodes for SOFC [8–11]. Among the many alternative electrode materials for SOFC, cobalt-containing $Sm_{0.5}Sr_{0.5}CoO_{3-\delta}$ (SSC) [12–14] and BSCF may be the two most popular materials due to their outstanding activity at reduced temperatures.

* Corresponding authors. Tel.: +86 25 83172256; fax: +86 25 83172242.
E-mail addresses: hj2007.park@samsung.com (H.J. Park), shaozp@njut.edu.cn (Z. Shao).

0378-7753/$ – see front matter © 2012 Elsevier B.V. All rights reserved.
doi:10.1016/j.jpowsour.2012.03.019

Long-term stability is an important issue for an electrode to be practically applicable. Although very low ASRs have been reported for both SSC and BSCF electrodes, their reliability for ORR has only rarely been reported, which may be related to the time-consuming nature of stability testing. Many doubts remain about the practicality of using cobalt-containing perovskites as cathodes in SOFCs because of their high thermal expansion coefficients (TECs) and unstable phase structure [15,16]. For example, SSC and BSCF electrodes were reported to have TECs of 20.5 and 20–25 $\times 10^{-6}\,K^{-1}$ (respectively) from room temperature to 1000 °C [17,18], much greater than those of $Sm_{0.2}Ce_{0.8}O_{1.9}$ (SDC) ($\sim 12.2 \times 10^{-6}\,K^{-1}$) or 8 mol% yttria-stabilized zirconia (YSZ) ($10.5 \times 10^{-6}\,K^{-1}$) electrolytes [19,20]. Such large TEC disparities may create significant internal stress in the fuel cell and result in the slow delamination of the cathode layer from the electrolyte's surface during operation. The performance of the electrode may therefore slowly decay with increasing operation time [21]. Regarding BSCF, a phase transition from a cubic perovskite phase to a hexagonal phase has been reported at temperatures lower than 850 °C [22]. This phase transition could decrease the bulk diffusion rate of oxygen and/or its surface exchange kinetics. Previously, when applying BSCF as a ceramic membrane, a gradual decrease of oxygen permeation flux with operation time has been observed at temperatures lower than 850 °C [23].

For cathodes of SOFCs used for power generation and for electrodes of symmetric cells used for activity evaluation, current collection is essential. Many different types of current collector materials and current collecting strategies have been studied in the literature [24–26]. Among the various current collector materials, silver has been extensively applied because of its relatively low price, high electronic conductivity and easy management. Previously, we demonstrated that both the materials and strategies used for current collecting can have significant effects on the area specific resistances (ASRs) of the electrodes for ORR [27].

In this study, the long-term operational stability of SSC and BSCF electrodes were specifically investigated using symmetric cell tests. Silver was selected as the current collector material, and two types of current collecting strategies were evaluated: whole electrode surface deposited with a diluted silver paste (CC-01) or a mesh-like silver collector using concentrated silver paste (CC-02). Interestingly, a BSCF electrode with the CC-01 current collector shows fairly stable performance within a test period of 800 h, as measured by the symmetric cell test. This finding suggests that the phase transition does not have an obvious effect on the performance of the BSCF electrode for ORR.

2. Experimental

2.1. Power synthesis and cell preparation

Oxide powders, including BSCF and SSC electrode materials and SDC electrolyte material, were all prepared with an EDTA–citrate complexing sol–gel process. During the synthesis, analytical reagents of metal nitrates were applied as the raw materials. Taking the preparation of SSC powder as an example, the required amounts of $Sm(NO_3)_2$, $Sr(NO_3)_2$ and $Co(NO_3)_2$, used without further treatment, were first mixed into an aqueous solution according to Sm:Sr:Co stoichiometry of 0.5:0.5:1. Then, both EDTA and citric acid were added to act as chelating agents, and the molar ratio of total metal ions to EDTA to citric acid was controlled at 1:1:2. If precipitation occurred during the gel preparation process, NH_4OH was used to adjust the pH of the system to allow a clear solution to re-appear. Under continuous heating and stirring, the water in the solution was slowly vaporized until a transparent gel was formed. The gel was then pre-treated at 250 °C for 3 h, converting it into a black-colored precursor, and then it was further calcined at 900 °C for 5 h in air to obtain a final product with the targeted phase composition.

Symmetric cells with an electrode |electrolyte| electrode configuration were fabricated for the evaluation of electrode activity and long-term performance stability test in this study. Disk-shape SDC pellets with a diameter of ~12 mm (after sintering) were used as the electrolytes; the pellets were dry pressed in a stainless steel die with a diameter of 15 mm and subsequently sintered in air at 1350 °C for 5 h. BSCF or SSC + SDC composite (weight ratio of 7:3) in powder form was well dispersed in a solution of glycerol, ethylene glycol and isopropyl alcohol to obtain a colloidal suspension, with the help of high-energy ball milling (Fritsch, Pulverisette 6) at 400 rpm for 0.5 h. This suspension was then deposited onto both sides of dense SDC pellets by an air-driven sprayer and then calcined at 1000 °C for 2 h in air to obtain complete symmetric cells with two identical porous electrodes on both sides of the SDC electrolyte.

Silver was used as the current collector. For the CC-01 current collection method, concentrated silver paste (DAD-87, Shanghai Research Institute of Synthetic Resins) was dispersed in liquid ethanol under ultrasonic vibration, and an appropriate amount of polyvinyl butyral was added to act as a pore former. The diluted silver paste was then painted onto the entire electrode's surface with a brush to form a thin silver paste layer of uniform thickness. For the CC-02 current collection method, a mesh-like morphological structure of concentrated silver paste was drawn with a stick directly onto the electrode surface to create the current collector, after which the electrode was fired at 180 °C for an hour. For symmetric cell tests, silver wires acting as connecting leads were attached to the above two current collectors with concentrated silver paste.

2.2. Characterization

Electrochemical impedance spectra (EIS) of the symmetric cells were measured using a Solartron 1260 Frequency Response Analyzer in combination with a Solartron 1287 potentiostat. The frequency used for the EIS measurements ranged from 10^{-1} to 10^5 Hz with a signal amplitude of 10 mV. Samples were tested under open circuit voltage (OCV) conditions. All tests of the symmetric cells were conducted under ambient air conditions. Microscopic features of the symmetric cell electrodes before and after the long-term stability tests were characterized by an environmental scanning electron microscope (E-SEM, Model QUANTA-200). The phase structure of the powders was characterized with an X-ray diffractometer (XRD, Bruker D8 Advance) equipped with Cu Ka radiation.

3. Results and discussion

Silver paste is often used as a current collector in SOFCs due to its high electronic conductivity and morphological flexibility. The most efficient means of current collection should involve contacting the whole electrode's surface with current collector. When applying concentrated silver paste as the current collector, however, the silver may become too dense due to sintering. Once the entire electrode surface is covered with concentrated silver paste, the poor porosity of the silver current collector may block free gas diffusion and thus induce concentration polarization. Indeed, we find previously that diluted silver paste combined with a pore former performed better than a concentrated silver paste current collector [27]. Thus, in this study, when the entire electrode surface is covered with silver paste to act as a current collector, a diluted form of silver paste is applied (CC-01). We also try another current collection method using silver paste, i.e., silver paste is applied with a mesh-like morphology onto the electrode surface (CC-02) in such a way that free gas diffusion could still be realized through

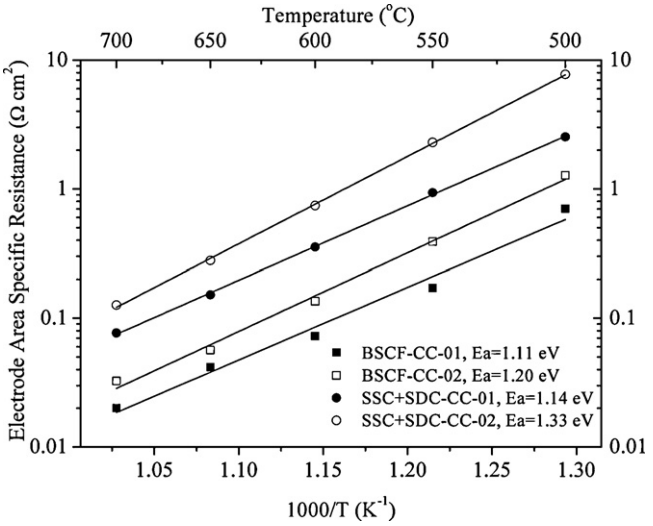

Fig. 1. Arrhenius plots of symmetric cells with BSCF and SSC + SDC as electrodes using silver paste (CC-01) and mesh-like silver (CC-02) as current collectors.

the electrode area lacking the silver paste even when the silver paste becomes highly dense. To achieve better adhesion of silver to the electrode's surface for the CC02 current collector, we apply concentrated silver paste.

To exploit the potential effect of these two different current collection methods on the performance of SSC and BSCF electrodes, the ASRs of a BSCF electrode and a SSC + SDC composite electrode with CC-01 and CC-02 current collectors (the morphologies of the current collectors will be presented later) are first comparatively studied at various temperatures, and the results are shown in Fig. 1. Much lower ASRs are observed for both the SSC and BSCF electrodes with the CC-01 current collection method than with CC-02. For example, the ASRs are 0.020, 0.042, 0.073, 0.17 and 0.70 $\Omega\,cm^2$ at 700, 650, 600, 550, 500 °C for the BSCF electrode using silver paste as the current collector, whereas the corresponding values are 0.033, 0.057, 0.14, 0.39 and 1.3 $\Omega\,cm^2$ using the mesh-like silver current collector. This finding suggests that whole-surface deposition with diluted silver paste is much more efficient than mesh-like current collection for these electrodes. This finding can be easily explained by the fact that part of the electrode surface is not covered with silver by applying the CC-02 current collector and that the electrical conductivity of porous electrodes, especially porous BSCF, is very low.

Considering the higher electrode performance achieved with the CC-01 current collection method, this method is first applied for the operational stability investigations of SSC and BSCF electrodes for ORR. Fig. 2 shows the dependence of ASR on time for both electrodes in ambient air. An obvious increase in electrode polarization resistance with operating time is observed for both electrodes. For example, the initial ASR is 0.107 $\Omega\,cm^2$ for the SSC + SDC electrode at 700 °C, and it increases to 0.149 $\Omega\,cm^2$ after operating for a period of 75 h, and further increases to 0.165 $\Omega\,cm^2$ after operating for 194 h. With regard to the BSCF electrode, the initial ASR is only 0.021 $\Omega\,cm^2$ at 700 °C, much lower than that of the SSC + SDC electrode, reflecting the much higher electrocatalytic activity of BSCF for ORR, as expected. However, the ASR also increases by 69% after continuous operation for approximately 363 h. The above results indicate that the performance of both the BSCF and SSC + SDC electrodes is unstable when using the CC-01 current collector with diluted silver paste covering the whole surface of the electrode.

Table 1
Fitting R_{ohm}, R_1 and R_2 values from EIS data of two symmetric cells with silver paste as current collector.

	SSC + SDC			BSCF		
	6 (h)	75 (h)	194 (h)	4 (h)	189 (h)	386 (h)
R_{ohm} ($\Omega\,cm^2$)	1.65	1.71	1.74	1.59	1.62	1.65
R_1 ($\Omega\,cm^2$)	0.0619	0.0789	0.0922	0.00106	0.00199	0.00501
R_2 ($\Omega\,cm^2$)	0.0600	0.0836	0.0922	0.0254	0.0301	0.0345

To obtain further insight into the deterioration of cell performance, selected representative EIS of symmetric cells with SSC + SDC and BSCF electrodes (Fig. 3) are analyzed in detail. An equivalent circuit of the mode L-R_{ohm}-(R_1-CPE_1)-(R_2-CPE_2) is adopted for the EIS data fitting, where L is the inductance originating from the connecting leads; R_{ohm} is an ideal resistor related to the ohmic resistance from the electrolyte, electrode, current collector and connecting leads; and CPE_i (constant phase element) represents a time-dependent capacitive element that is in parallel with the resistance marked R_i. The (R_1-CPE_1) is applied to fit the high-frequency region, and it primarily represents charge-transfer processes, including both electron-transfer and ion-transfer processes, occurring at the current collector/electrode and electrode/electrolyte interfaces [28]. The (R_2-CPE_2) is applied to fit the low-frequency region, and it primarily represents diffusion processes, including the adsorption–desorption of oxygen, oxygen diffusion at the gas – cathode interface, and surface diffusion of intermediate oxygen species [29]. The representative EIS are found to fit well with the above equivalent circuit, and the values of R_{ohm}, R_1 and R_2 are summarized in Table 1. For both electrodes, R_1 and R_2, which are related to charge-transfer and surface diffusion processes, respectively, increase with operating time. Interestingly, with increasing operating time, the R_{ohm} for the symmetric cell

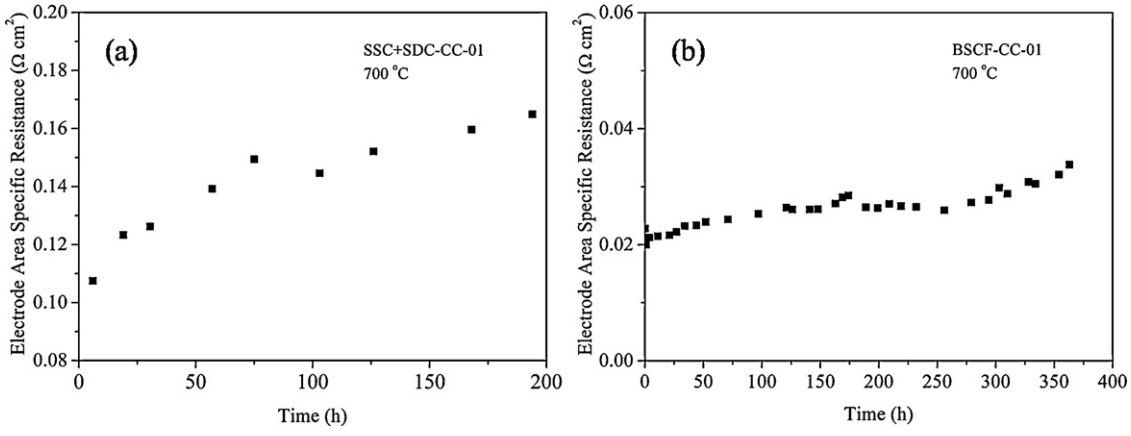

Fig. 2. Time-dependence of the ASRs of SSC + SDC (a) and BSCF (b) electrodes at 700 °C with CC-01 silver current collector.

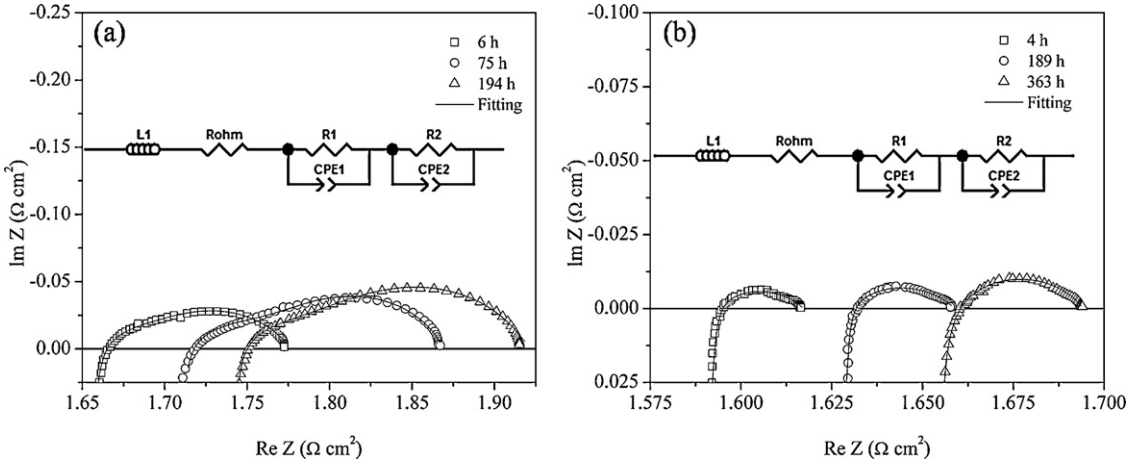

Fig. 3. Selected EIS data and corresponding fitting results for symmetric cells with SSC + SDC (a) or BSCF (b) electrodes applying CC-01 current collectors; the insets show the equivalent circuits used for fitting the EIS data.

with the SSC + SDC electrode also increases from an original value of 1.65 Ω cm^2 to 1.74 Ω cm^2 after continuous operation for a period of approximately 200 h. A similar increase in R_{ohm} with operating time is also observed for the symmetric cell with the BSCF electrode.

It has been reported that SSC has a stable phase structure under the operating conditions of an SOFC cathode [17]. This finding is further supported in our study by comparing the XRD patterns of fresh SSC, SDC (SSC-fresh, SDC-fresh) and 400 h sintered SSC + SDC (SSC + SDC-400 h), as shown in Fig. 4. This comparison reveals that the performance deterioration of the SSC + SDC electrode, as demonstrated in the symmetric cell test using the CC-01 silver current collector, is less likely due to the progressive phase transition of the electrode during the duration test. Delamination between the electrode and the electrolyte's surface, typically originating from thermal expansion disparity between electrode and electrolyte, is believed to be one of the main causes of performance deterioration for many electrodes, in particular for cobalt-containing perovskite oxide electrodes. As mentioned previously, the TECs of BSCF and SSC are much larger than that of SDC. To determine whether internal stress caused by the different TECs of the SSC electrode and the SDC electrolyte leads to the performance of the electrode to deteriorate, the symmetric cells with SDC + SSC electrodes and SDC electrolyte before and after continuous operation for a period of 194 h in air at 700 °C are examined by SEM. Shown in Fig. 5 are cross-sectional SEM images of the interfaces between the SSC + SDC

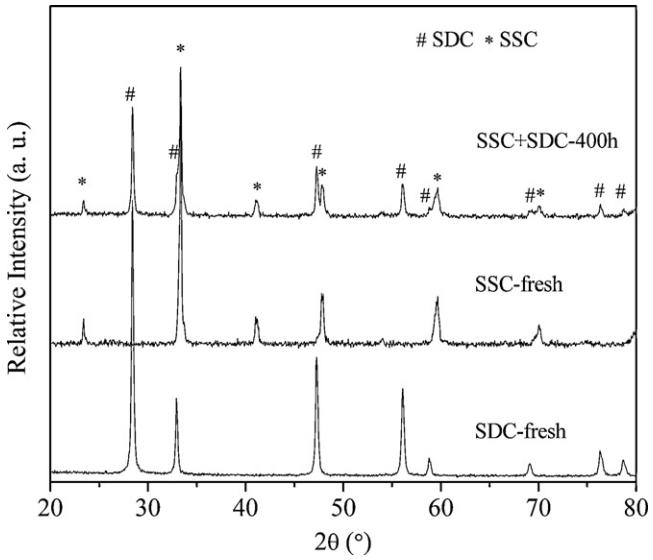

Fig. 4. XRD patterns of SSC, SDC and SSC + SDC mixtures before and after calcination at 700 °C for 400 h.

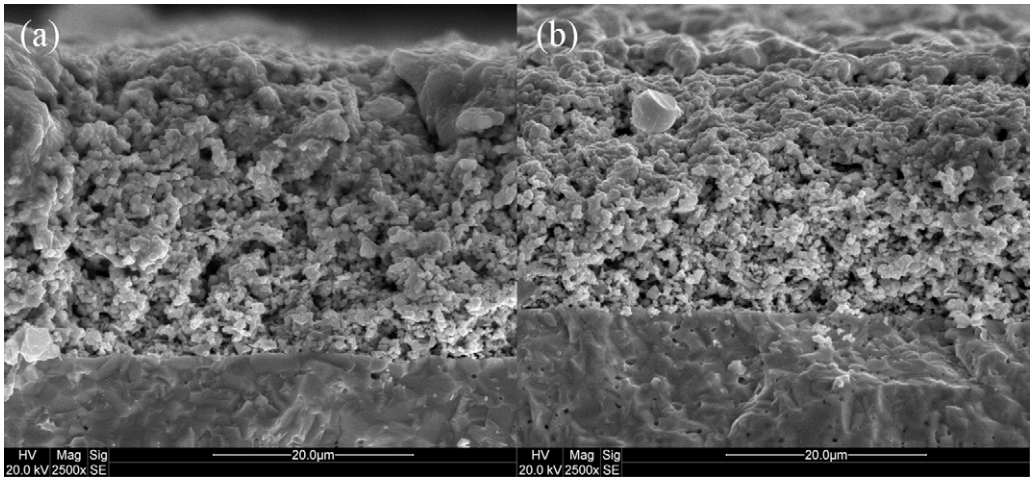

Fig. 5. SEM images of the interface between an SSC + SDC electrode and SDC electrolyte before (a) and after (b) 194 h of long-term testing at 700 °C from a cross-sectional view of SSC + SDC|SDC|SSC + SDC symmetric cells.

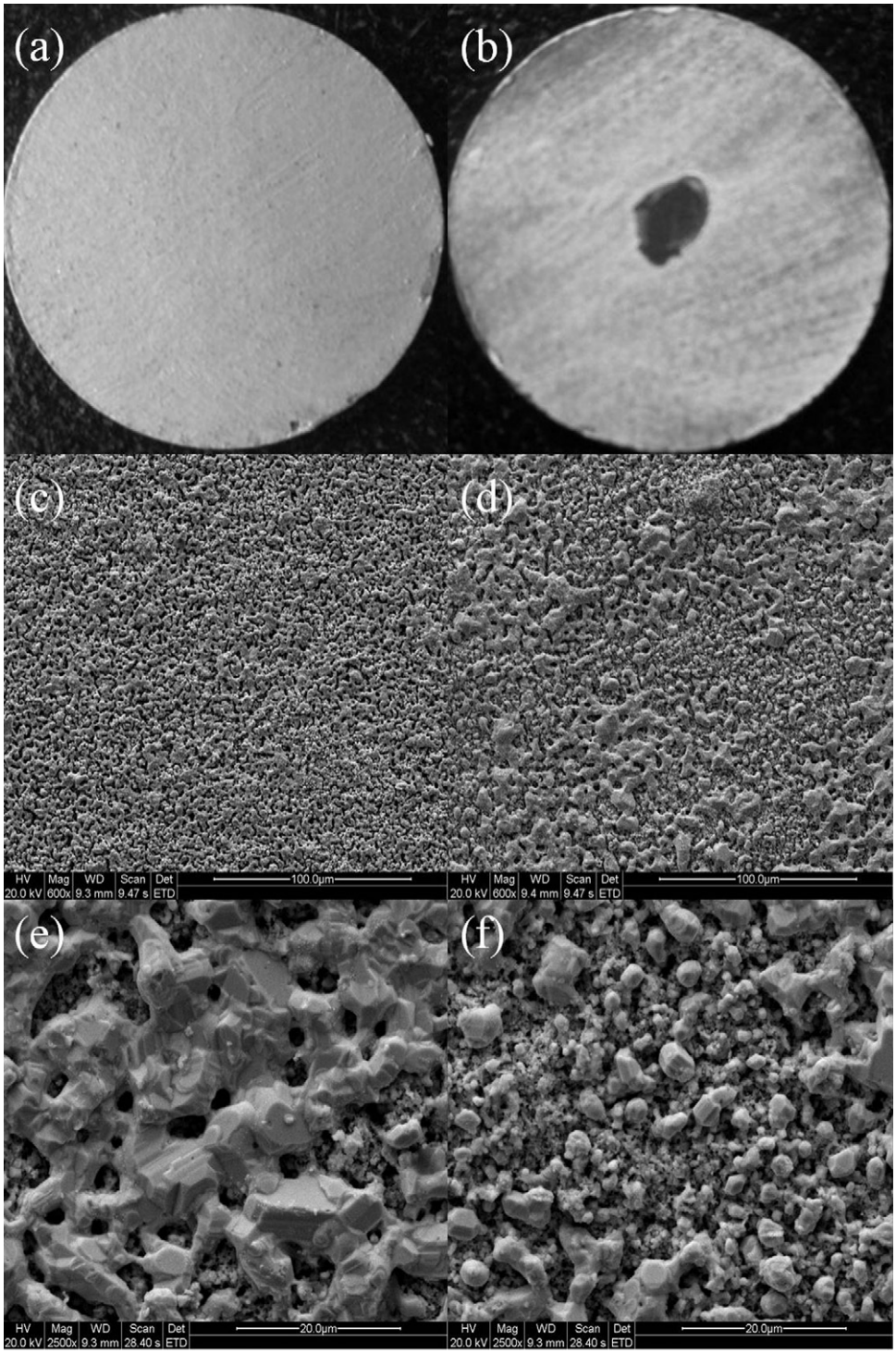

Fig. 6. Digital photos and SEM images of a silver paste current collector before (a, c) and after (b, d, e, f) a stability test for 194 h.

electrode and SDC electrolyte before and after long-term stability testing. Interestingly, no obvious delamination of the SSC + SDC electrode layer from the SDC electrolyte is detected. This finding strongly implies that delamination of the electrode layer from the SDC electrolyte during stability testing is not a practical problem for SSC + SDC electrodes. The good interfacial stability of the SSC + SDC| SDC can then be explained as follows. On the one hand, the porous nature of SSC + SDC electrodes effectively buffers the internal stress induced by the disparity in TECs between the electrode and the electrolyte during the heating process. On the other hand, the difference in the absolute value of the dimensional change between the SSC + SDC electrode and SDC electrolyte is still small due to the relatively low operating temperature (700 °C) in this study. Similarly, no obvious delamination of the BSCF electrode from the SDC electrolyte is observed (data not shown) after the stability test. Thus, the TEC disparity between SSC + SDC and BSCF electrodes and SDC electrolyte is less likely to be a practical problem in SOFCs operated at intermediate temperature, at least in this study. Moreover, oxygen ion-transfer at the electrode/electrolyte interface is found not to be the origin of the performance deterioration of either

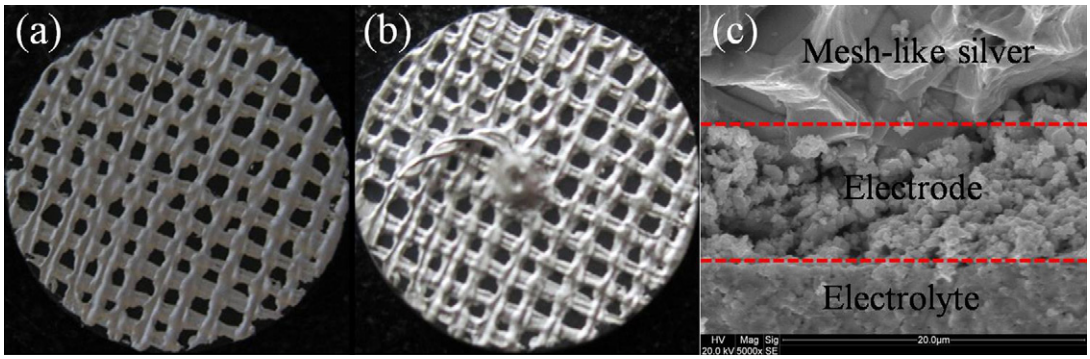

Fig. 7. Digital photos of a typical SSC + SDC electrode with the CC-02 mesh-like silver current collector before (a) and after (b) 450 h of operation, and an SEM image of an SSC + SDC electrode from a cross-sectional view (c).

SSC + SDC| SDC| SSC + SDC or BSCF| SDC| BSCF symmetric cells with CC-01 current collectors.

Comparing digital photos of silver paste current collectors before and after long-term stability testing (Fig. 6a and b) reveals significant morphological changes of the current collector. The silver paste current collector appears to have evaporated markedly after long-term operation. Fig. 6c–f presents more detailed information about the silver paste current collector before and after long-term stability testing. Fig. 6c shows that the silver paste initially exhibits a well-connected and porous structure that uniformly covers the electrode's surface. However, as shown in Fig. 6d–f, the initial morphological structure of the silver paste current collector is largely destroyed after the stability test due to sintering and evaporation of the silver. Sintering of the silver current collector may block free gas transportation, and evaporation of the silver may reduce its current collection efficiency. Both processes likely contribute to the performance deterioration of the SSC + SDC and BSCF electrodes in ORR. Increases in R_{ohm} and R_1, as demonstrated previously, may be caused by reduced current collection efficiency, whereas increases in R_2 may be caused by reduced gas diffusion.

Considering the rapid evaporation of silver from the porous CC-01 silver current collector due to the large exposed surface area, we also adopt a dense mesh-like silver current collector (CC-02) for the SSC + SDC symmetric cell and investigate its stability. It has been reported that the evaporation of silver from dense silver mesh during long-term testing at 690 °C under air is slight [30]. Thus, morphological changes of the current collector should be minimized by adopting the CC-02 method during the stability test, although the ASR of the electrode may be larger than that when applying the CC-01 method. Digital photos of a typical SSC + SDC electrode with the mesh-like silver current collector before and after long-term operation are shown in Fig. 7a and b. Indeed, the silver mesh retains its original morphology after long-term operation. Cross-sectional SEM images of a symmetric cell with an SSC + SDC electrode and the silver mesh current collector are presented in Fig. 7c, demonstrating that the current collector adhere to the electrode's surface quite well after long-term operation without any appearance of delamination. This finding further demonstrates that the large difference in TECs between the SSC + SDC electrode and the SDC electrolyte is not a serious problem because of the reduced operating temperature and the porous electrode structure.

The time dependence of the ASR of an SSC + SDC electrode using a mesh-like silver current collector (CC-02) is shown in Fig. 8. Interestingly, the electrode's polarization resistance is fairly stable with respect to operating time within the test period of approximately 450 h. The ASR is found to fluctuate at approximately 0.15 Ω cm^2 within the whole test period, and this fluctuation is likely due to the temperature variation during the operation. The above results

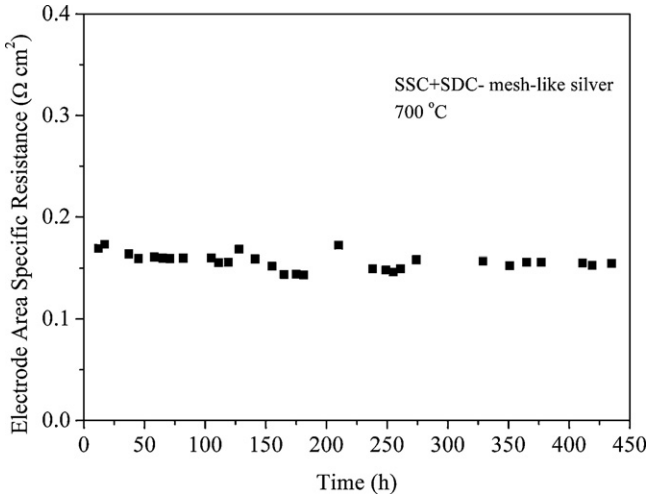

Fig. 8. Time-dependence of the ASRs of an SSC + SDC electrode at 700 °C with a CC-02 mesh-like silver current collector.

further indicate that the SSC + SDC electrode by itself is highly stable, and the deterioration of the cell's performance when adopting the CC-01 current collector is caused by sintering and evaporation of the silver paste.

It is generally accepted that BSCF has very high activity for ORR at intermediate temperatures due to its high oxygen ionic conductivity and oxygen surface exchange properties [31,32], which are due to the high oxygen vacancy concentration and also the high oxygen mobility within the bulk of BSCF. It has also been demonstrated that surface diffusion is the rate-limiting step for ORR in a BSCF electrode [33,34]. However, the large TEC and poor phase stability of BSCF have become major roadblocks to its potential application in SOFCs operated at intermediate temperature. The above studies suggest that high TEC may not be a serious problem, at least for the application of such electrodes in SOFCs operated at intermediate temperature, because of the low operating temperature (<800 °C) and the porous electrode morphology. However, phase structure stability remains a primary concern.

The oxygen permeation stability of BSCF ceramic membrane is first reported by Shao et al. [23]. They demonstrate that stable oxygen permeation can be obtained only at operation temperatures higher than 850 °C, and permeation flux slowly deteriorates with operating time at temperatures below that, an effect ascribed to gradual phase decomposition/transformation. However, it is suggested that the phase structure can be recovered by re-treating the membrane at temperatures higher than 850 °C for a sufficient length of time [23]. Švarcová et al. find that after long-term

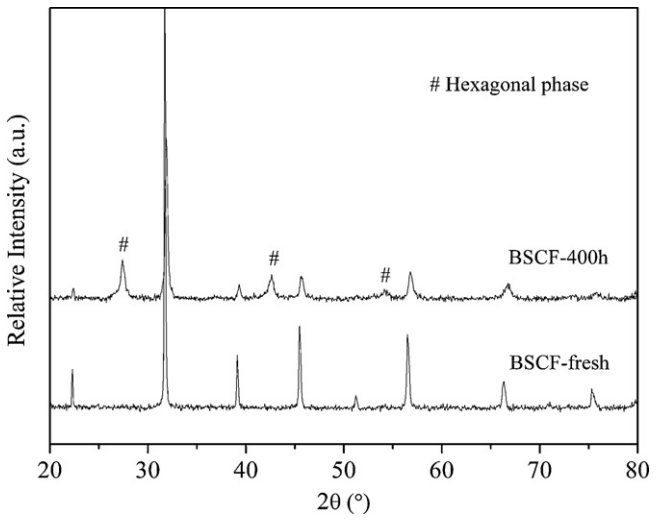

Fig. 9. XRD results from BSCF powder before and after 400 h of calcination at 700 °C under ambient air.

annealing of BSCF powders, a hexagonal perovskite structure can be detected with XRD [22]. Arnold et al. further explain that cobalt instability leads to the decomposition of perovskite from cubic to hexagonal via an unknown monoclinic phase at intermediate temperatures [35]. With TEM, Efimov et al. discover several micrometer-long lamellae with a low concentration of mobile oxygen vacancies in the structure of $Ba_{1-x}Sr_xCo_{2-y}Fe_yO_{5-\delta}$, which are likely to serve as barriers to oxygen transportation [36]. The decomposition kinetics of BSCF from cubic to hexagonal structure is also studied by Mueller et al. [37]. To examine the phase stability of BSCF in our study, it is calcined at 700 °C in air for 400 h without polarization (BSCF-400 h). Fig. 9 shows the XRD spectra of various samples. Fresh BSCF (BSCF-fresh), prepared by calcination at 1000 °C in air, displays a perovskite structure well indexed as cubic symmetry with a Pm-3m space group. However, after calcination in air at 700 °C for 400 h, a phase transition is observed.

The performance stability of BSCF electrodes for ORR is further investigated by symmetric cell testing using mesh-like silver as the current collector for a total period of 800 h in ambient air. Fig. 10 shows the ASR of the BSCF electrode as a function of operation time. Surprisingly, the overall ASR is fairly stable, retaining a value of 0.065 Ω cm^2 during 800 h of continuous operation, although a fluctuation of the ASR value is observed, mainly in the range of 0.06–0.07 Ω cm^2, which can be assigned to temperature variation during the experiment. This result suggests that BSCF can perform stably as an oxygen reduction electrode even though a phase transition is found to occur during long-term operation, implying that the products from the phase transition still show very good electrocatalytic activity for ORR. Previously, we demonstrated that the ORR over the BSCF electrode is mainly limited by the surface diffusion of oxygen [7]. This consideration strongly suggests that the surface exchange kinetics of BSCF electrode is less likely to be affected after the phase transition. Even though the final transition has effects after sufficiently long operation times, the phase structure can be restored by heating the electrode to a temperature higher than 850 °C. In addition, the BSCF cathode is also sensitive to the CO_2 which could also cause the decay of the performance of BSCF. In this study, it seems the traces of CO_2 in ambient air did not cause the poisoning effect. Thus, BSCF is a promising electrode for ORR at intermediate temperatures.

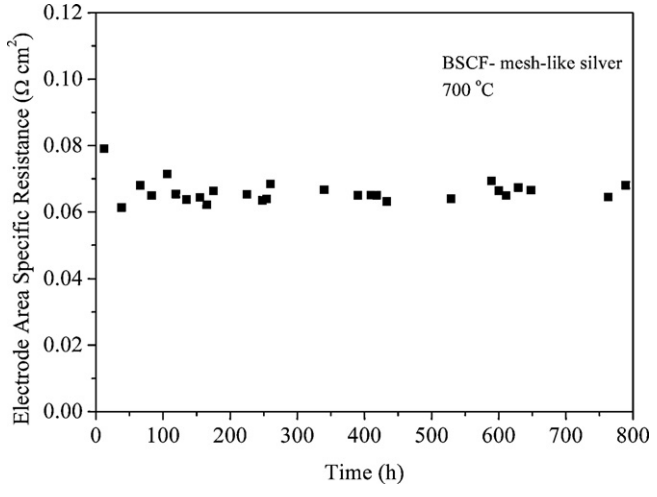

Fig. 10. ASR values of a BSCF electrode as a function of operating time at 700 °C with a CC-02 mesh-like silver current collector.

4. Conclusions

In this study, by applying mesh-like dense silver as the current collector, we obtained long-term stable performance with both BSCF and SSC + SDC electrodes. Using the appropriate current collector is crucial to achieving such stable electrode performance. Although diluted porous silver paste showed better current collection efficiency than mesh-like silver, thus providing higher initial electrode performance, the porous morphological structure of the silver current collector was largely destroyed after the long-term stability test because of silver sintering and evaporation, which caused progressive deterioration of the electrode's performance. By contrast, the mesh-like silver current collector exhibited a fairly stable structure during the long-term stability test. Thus, gas diffusion was not impacted and current collection efficiency was maintained. Although BSCF experienced a phase transition at reduced temperatures, fairly stable electrode performance was still achievable with this material. The phase transition did not have a great effect on oxygen reduction over the BSCF electrode.

Acknowledgements

This work was supported by the "National Science Foundation for Distinguished Young Scholars of China" under contract No. 51025209 and also the Samsung Advanced Institute of Technology.

References

[1] B.C.H. Steele, J. Mater. Sci. 36 (2001) 1053–1068.
[2] D.J.L. Brett, A. Atkinson, N.P. Brandon, S.J. Skinner, Chem. Soc. Rev. 37 (2008) 1568–1578.
[3] E.P. Murray, T. Tsai, S.A. Barnett, Solid State Ionics 110 (1998) 235–243.
[4] K. Sasaki, J. Tamura, H. Hosoda, T.N. Lan, K. Yasumoto, M. Dokiya, Solid State Ionics 148 (2002) 551–555.
[5] S.B. Adler, Chem. Rev. 104 (2004) 4791–4843.
[6] W. Zhou, F.L. Liang, Z.P. Shao, J.L. Chen, Z.H. Zhu, Sci. Rep. 1 (2011) 155.
[7] Z.P. Shao, S.M. Haile, Nature 431 (2004) 170–173.
[8] C. Huang, D.J. Chen, Y. Lin, R. Ran, Z.P. Shao, J. Power Sources 195 (2010) 5176–5184.
[9] H.L. Zhao, W. Shen, Z.M. Zhu, X. Li, Z.F. Wang, J. Power Sources 182 (2008) 503–509.
[10] Q. Liu, X.H. Dong, G.L. Xiao, F. Zhao, F.L. Chen, Adv. Mater. 22 (2010) 5478–5482.
[11] D.J. Chen, R. Ran, Z.P. Shao, J. Power Sources 195 (2010) 7187–7195.
[12] T. Hibino, A. Hashimoto, T. Inoue, J. Tokuno, S. Yoshida, M. Sano, Science 288 (2000) 2031–2033.
[13] J.D. Nicholas, S.A. Barnett, J. Electrochem. Soc. 157 (2010) B536–B541.
[14] Y.M. Guo, D.J. Chen, H.G. Shi, R. Ran, Z.P. Shao, Electrochim. Acta 56 (2011) 2870–2876.
[15] A.J. Jacobson, Chem. Mater. 22 (2010) 660–674.
[16] H. Ullmann, N. Trofimenko, Solid State Ionics 119 (1999) 1–8.
[17] H.Y. Tu, Y. Takeda, N. Imanishi, O. Yamamoto, Solid State Ionics 100 (1997) 283–288.
[18] B. Wei, Z. Lv, X.Q. Huang, J.P. Miao, X.Q. Sha, X.S. Xin, W.H. Su, J. Eur. Ceram. Soc. 26 (2006) 2827–2832.

[19] K. Eguchi, T. Setoguchi, T. Inoue, H. Arai, Solid State Ionics 52 (1992) 165–172.
[20] O. Yamamoto, Electrochim. Acta 45 (2000) 2423–2435.
[21] K. Park, S. Yu, J. Bae, H. Kim, Y. Ko, Int. J. Hydrogen Energy 35 (2010) 8670–8677.
[22] S. Švarcová, K. Wiik, J. Tolchard, H.J.M. Bouwmeester, T. Grande, Solid State Ionics 178 (2008) 1787–1791.
[23] Z.P. Shao, W.S. Yang, Y. Cong, H. Dong, J.H. Tong, G.X. Xiong, J. Membr. Sci. 172 (2000) 177–188.
[24] C.E. Hatchwell, N.M. Sammes, K. Kendall, J. Power Sources 70 (1998) 85–90.
[25] K.C.R.D. Silva, B.J. Kaseman, D.J. Bayless, Int. J. Hydrogen Energy 36 (2011) 779–786.
[26] J.H. Kim, R.H. Song, D.Y. Chung, S.H. Hyun, D.R. Shin, J. Power Sources 188 (2009) 447–452.
[27] Y.M. Guo, Y.B. Zhou, D.J. Chen, H.G. Shi, R. Ran, Z.P. Shao, J. Power Sources 196 (2011) 5511–5519.
[28] S.B. Adler, Solid State Ionics 135 (2000) 603–612.
[29] W. Zhou, B.M. An, R. Ran, Z.P. Shao, J. Electrochem. Soc. 156 (2009) B884–B890.
[30] W.A. Meulenberg, O. Teller, U. Flesch, H.P. Buchkremer, D. Stover, J. Mater. Sci. 36 (2001) 3189–3195.
[31] S. Mcintosh, J.F. Vente, W.G. Haije, D.H.A. Blank, H.J.M. Bouwmeester, Chem. Mater. 18 (2006) 2187–2193.
[32] D.J. Chen, Z.P. Shao, Int. J. Hydrogen Energy 36 (2011) 6948–6956.
[33] W. Zhou, R. Ran, Z.P. Shao, J. Power Sources 192 (2009) 231–246.
[34] F.S. Baumann, J. Fleig, H.U. Habermeier, J. Maier, Solid State Ionics 177 (2006) 3187–3191.
[35] M. Arnold, Q. Xu, F.D. Tichelaar, A. Feldhoff, Chem. Mater. 21 (2009) 635–640.
[36] K. Efimov, Q. Xu, A. Feldhoff, Chem. Mater. 22 (2010) 5866–5875.
[37] D.N. Mueller, R.A.D. Souza, T.E. Weirich, D. Roehrens, J. Mayer, M. Martin, Phys. Chem. Chem. Phys. 12 (2010) 10320–10328.